Available online at www.eccomasproceedia.org
Eccomas Proceedia SMART (2023) 379-389

ECCOMAS
Proceedia

X ECCOMAS Thematic Conference on Smart Structures and Materials
SMART 2023
D.A. Saravanos, A. Benjeddou, N. Chrysochoidis and T. Theodosiou (Eds)

FABRICATION AND CHARACTERIZATION OF A SHAPE MEMORY ALLOY DRIVEN COMPOSITE MORPHING RADIATOR PROTOTYPE

Priscilla Nizio* **and Darren Hartl***

*Texas A&M University
Department of Aerospace Engineering
701 H.R. Bright Building 3141, College Station, TX 77843
e-mail: darren.hartl@tamu.edu

Key words: Shape memory alloy, Radiator, Experimental validation

Abstract. The extreme environment of deep space requires thermal control capable of maintaining safe temperatures within the spacecraft. In the vacuum of space, radiation is the dominant heat transfer mechanism for rejecting waste heat. Radiators incorporated within a thermal control system (TCS) enable temperature adjustments to the TCS working fluid loop. Shape adaptive morphing radiators control the TCS working fluid temperature partially through radiator geometry modifications, enabling variable heat rejection capabilities and possibly eliminating the need for multiple fluid loops, therefore decreasing system mass. The 2015 NASA Technology Roadmap dictates that the ratio between the maximum and minimum heat rejection, known as the turndown ratio, be at least 6:1 to manage changing thermal requirements between low Earth orbit, interplanetary travel, and lunar surface operations. Components formed from shape memory alloys (SMAs) change shape in response to a thermal stimulus. In this work, SMA wires are wrapped around an open cylindrical conductive composite shell and are conductively coupled to coolant passages, providing thermally responsive actuation that opens and closes the composite radiator at design temperatures. The carbon fiber radiator facesheet optimizes both thermal conductivity and stiffness properties, allowing for enhanced thermal and structural performance, respectively. The SMA wire transformation temperatures and actuation properties are tailored to the requirements of a specific mission, and heat rejection adaptability is demonstrated. While past prototypes have proven concept feasibility in a relevant thermal environment, this work considers the most high-performance and carefully designed morphing radiator to date increasing the technology readiness level (TRL) to TRL 5.

1 INTRODUCTION

The Artemis and future interplanetary missions require innovative technologies to withstand the harsh and changing environment of space. NASA's 2015 technology roadmap calls for variable-geometry radiators with turndown ratios of at least 6:1 and a stretch goal of 12:1 [1]. Turndown is the ratio of the maximum and minimum heat rejection capabilities of the TCS, and

Peer-review under responsibility of the organizing committee of SMART 2023.
doi: 10.7712/150123.9793.444712

is typically used to quantify performance. A turndown radiator modulates the heat rejection from the TCS to ensure that certain system temperatures are maintained within desired levels. A reduction in the heat rejection, or turndown, of a radiator can be achieved by changing the radiators optical properties (related to thermal radiation efficiency), the temperature (related to the coolant being supplied to the radiator), the environment (related to the radiators view to the sun or deep space), or the shape (related to the radiating surface area) [2]. In the present work, shape memory alloys (SMAs) are applied to a thermal radiator to deform the radiator in response to its temperature. This provides turndown in response to heat rejection and environmental conditions, requiring no external power for actuation or control.

The working fluid from a TCS collects heat from the spacecraft (electronics, life support systems, etc), flows through radiators, and allows heat to be rejected to space via radiation, decreasing the working fluid temperature, as depicted in Figure 1a. Low heat loads or cold environments increase risk that the radiator surface temperature decreases below the freezing point of the working fluid. To mitigate this, the fluids used in TCS areas subjected to low temperature environments are limited to those with low freezing points.

Current human spaceflight architecture utilize a dual-loop system that separates the internal loop and external loop, and allows two different fluids to be used in the TCS. A non-toxic fluid is required to be used in the inner loop where crew members may be present, and an often toxic low freezing point fluid is used outside of the enclosure. Heat between the two loops is interchanged through a heat exchanger, as shown in Figure 1a. Crewed vehicles such as Shuttle and ISS use a dual loop TCS architecture [3].

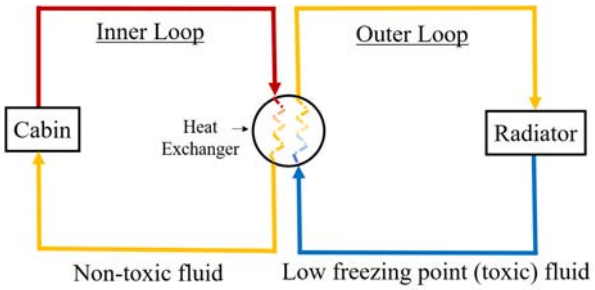

(a) Dual Loop TCS

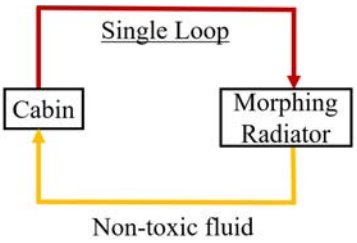

(b) Single Loop TCS

Figure 1: Comparison between a single and dual loop thermal control system architecture.

The change from a dual loop to a single loop system could reduce launch mass by approximately 23% as it would remove the need for the hardware necessary for the second loop, depicted in Figure 1 [4]. A single loop TCS architecture is depicted in Figure 1b, where morphing composites including thermally responsive materials prevent fluid freezing by enabling variable heat rejection. This mitigates the risk of toxic fluid interference with crew members by not restricting the working fluid to low freezing point fluids. State-of-the-art non-toxic thermal control system working fluids have freezing points above typical environmental temperatures of low Earth orbit (LEO) and beyond [4]. Although there is ongoing research on thermal control system working fluids in efforts to adapt non-toxic fluids to fit the necessary mission parameters, current single loop radiator technologies are limited to a small operating range, lessening its desirability given the modern spacecraft demands and current mission parameters [4].

The morphing radiator allows a non-toxic fluids in a single loop TCS architecture, preventing freezing by controlling the heat transfer into and out of the fluid without external controls. Figure 2 depicts the actuation of a morphing radiator, where in this case the passive actuation is possible through Shape Memory Alloys (SMAs). SMAs are a type of alloy able to undergo a temperature activated phase transformation between two solid phases, austenite and martensite. Austenite is the high temperature phase, and martensite is the low temperature phase. This transformation occurs by shear lattice distortion [5].

Previous works investigated using stainless steel foil adhered to thermal graphite sheets with SMA wires [6], a thermally conductive copper panel with SMA wires [7], and a composite facesheet with SMA strips [8]. This present work extends the development of the radiator prototype by using a carbon fiber composite facesheet, two different SMAs tailored to the lunar environment, and expanding operation to a five-panel serial subsystem.

2 THEORY OF OPERATION

SMA wires are wrapped around an open cylindrical conductive shell and are conductively coupled to coolant passages, providing thermally responsive actuation that opens and closes the composite radiator at design temperatures. Figure 2 depicts the concept of operations in a coupled five-panel system where the radiators are open for warm working fluid temperatures and gradually close as the working fluid cools, reducing heat rejection. Endcaps between each panel further reduce the view to deep space when the radiator is closed. The radiator size may be scaled to meet different mission requirements [9].

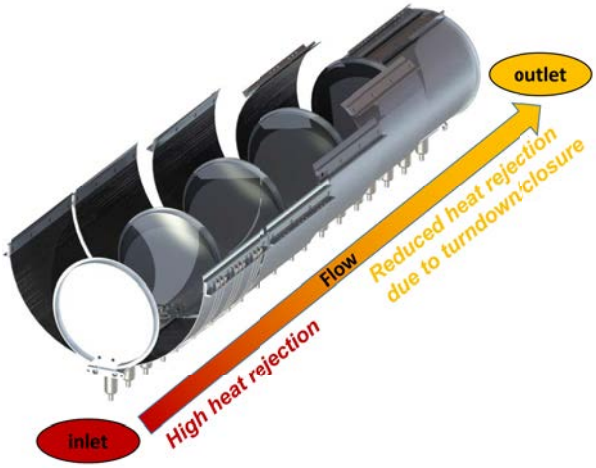

Figure 2: Morphing radiators coupled in a 5-panel system depicting the concept of operation [9]; color scheme consistent with Figure 1.

In the vacuum of deep space, heat is transferred through radiation, therefore the heat rejection rate $\dot{Q}$ can be estimated for an isothermal radiator of area A using the Stefan-Boltzmann Law,

$$\dot{Q} = \epsilon \sigma A F (T_s^4 - T_\infty^4), \tag{1}$$

where ϵ denotes the emissivity, σ denotes the Stefan–Boltzmann constant, F is defined as the fraction of heat leaving the surface that is absorbed by the surrounding space environment (also called the view factor), and T denotes the homogeneous surface temperature (T_s), and the environment (T_∞) [2]. This equation demonstrates the combined effect of the view factor exposed area, and exposed emissivity on the total heat rejection.

As more of the concave surface of the panel is exposed to space during high heat load environments, more heat is rejected (i.e. the view factor to space increases and the high emissivity carbon fiber panel is exposed). As the panel is closed during low heat load environments, the view factor decreases and heat rejection becomes dependent on the emissivity of the exposed

outer surface of the radiator, which is covered in Multi Layer Insulation (MLI) and is a poor emitter. The turndown ratio (R) can be calculated using the maximum and minimum heat rejection rates of the radiator, estimated by the Stefan-Boltzmann Law:

$$R = \frac{\dot{Q}_{max}}{\dot{Q}_{min}}. \tag{2}$$

In warm thermal environments, the SMA wires are in the austenite phase and behave elastically, pulling open the composite panels as depicted via the radiator positioned at the inlet of Figure 2. As the temperature of the working fluid cools, the SMA wires transition into oriented martensite as the mechanical stress of the facesheet elongates the wires, and allows the radiator to close as depicted via the radiator positioned at the outlet of Figure 2. When the working fluid temperature increases beyond the austenite start temperature, the SMA wires begin to transition into austenite, contracting and pulling the radiator panel back open. As the panel opens, more heat is rejected, cooling the working fluid. The SMA transition temperatures must be properly tuned to provide actuation at the correct temperatures and maintain the desired coolant temperature depending on mission requirements.

3 RADIATOR PANEL

The assembled structure needs to be capable of variable geometry, be highly thermally conductive, and be lightweight compared to conventional materials. Sufficient stiffness is needed to provide a biasing force to return the radiator to a fully closed configuration, sufficient compliance is needed to deform the radiator to an open configuration without failure, and adequate thermal conductivity is needed to transport heat out of fluid loop. Carbon fiber-reinforced composites are preferable for this application as their properties meet such requirements. A pre-impregnated unidirectional composite tape procured from Toray Industries and comprised of RS-3C resin and K13C2U pitch carbon fibers was chosen for this application. This material system satisfies spaceflight outgassing requirements and provides out-of-autoclave curing. Previous efforts used a similar, yet thinner composite system. However, that material system was not available in the appropriate project timeline [8]. For this effort, the new material system had to be characterized, and the new radiator panels built and tested.

(a) 4-Point bend experimental setup.

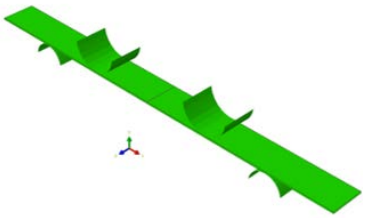

(b) 4-Point bend model setup.

Figure 3: 4-Point bend experimental and model setups.

3.1 COMPOSITE CHARACTERIZATION

The morphing radiator is modeled in the finite element analysis software Abaqus. A custom framework developed in previous efforts that allow for both thermal and structural analyses

was further developed to account for the new material systems [10] [11]. The K13C2U/ RS-3C system properties were experimentally characterized through a series of 4-point bend tests guided by ASTM D627217 using a set up as depicted in Figure 3a. An Abaqus model that mimics the experimental setup depicted in Figure 3b was used for calibration and validation of the material system.

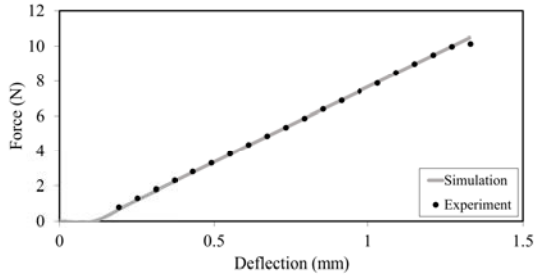

(a) [0/0/0/0] Composite layup for characterization of fiber direction.

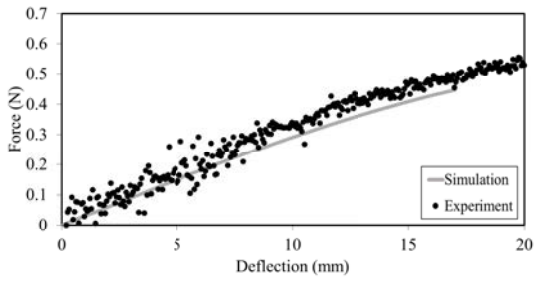

(b) [90/90/90/90] Composite layup for characterization of matrix direction.

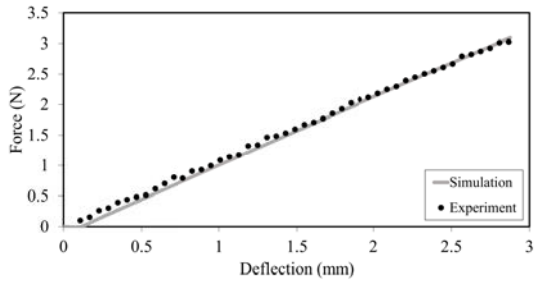

(c) [90/0/0/90] Composite layup for validation.

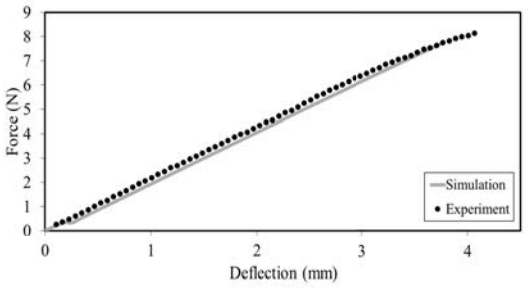

(d) [90/45/0/0/45/90] Composite layup for validation.

Figure 4: 4-Point bend force-displacement experimental tests, model calibration, and validation results (0.1 mm/s, 25 °C).

A simulation was carried out for a variety of different composite layups, and composite moduli were adjusted to match experimental force-displacement, depicted in Figure 4. [0/0/0/0] and [90/90/90/90] layups were used for model calibration, and [90/0/0/90] and [90/45/0/0/45/90] layups were used for validation. The shear modulus was also calibrated and aligns with literature values for graphite-epoxy shear modulus properties. The validated material properties are as described in Table 1, and are utilized in the morphing radiator model.

Table 1: Calibrated material properties of K13C2U/RS-3C.

E_{11}	335 GPa
E_{22}	2.45 GPa
G_{12}	4.66 GPa

Additional 4-point bend experiments performed at slow (0.1 mm/s) and accelerated (1 mm/s) rates, as well as in cold (-30 °C) and warm (25 °C) environments confirmed that neither the expected thermal environment nor actuation rate would have an adverse effect on the composite

response, allowing the possibility of accelerated laboratory testing at conventional room temperature. Figure 5a depicts matching material responses for differing testing rates, and 5b depicts matching material responses for differing test environmental temperatures.

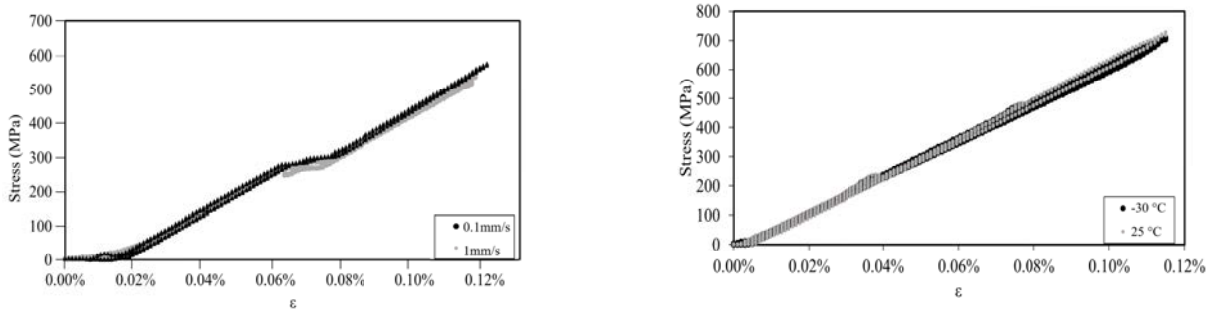

(a) Rate dependence test

(b) Temperature dependence test.

Figure 5: 4-Point bend stress vs. strain results for [0/0/0/0] composite layup differing test rate and temperature.

3.2 COMPOSITE PANEL FATIGUE TESTING

The fatigue life of the radiator panel is a primary design concern. A test stand constructed to scope and validate fatigue performance of the composite radiator panel included a motor, load cell, and rotary potentiometers on each side of the radiator. As depicted in Figure 6, the composite panel is mounted atop a prototype TCS interface to mimic realistic radiator actuation. Kevlar strings are used to open the radiator mechanically instead of SMA for simplicity, and are wrapped around a rod connected to the motor as well as attached to the tips of the panel. The motor turns the rods, pulling the panel open. The force required to open the panel is measured by the load cells, and the position of the panel is controlled by the rotary potentiometers. Combined with a custom-designed controller and data logging at 150 measurements per cycle, this setup quantifies any decrease in panel stiffness over time.

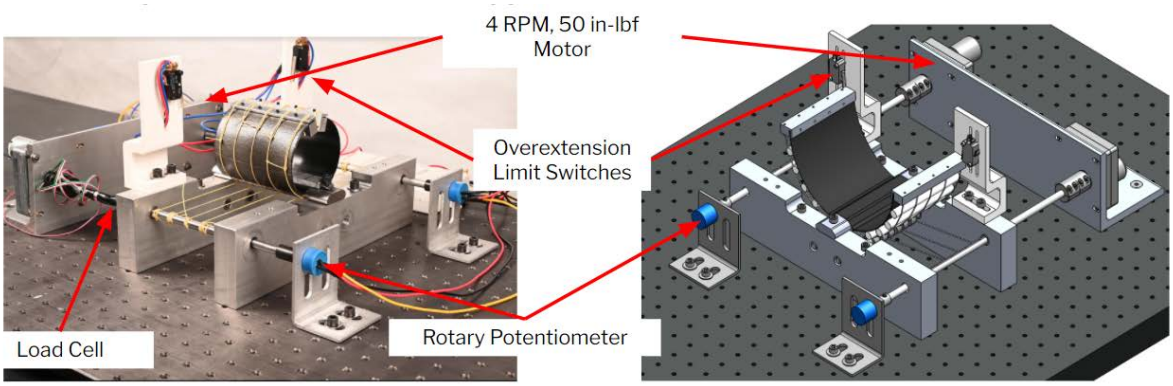

Figure 6: As built fatigue test stand (left). Modeled fatigue test stand (right).

As depicted in Figure 7, the radiator panel can survive full actuation strains for over 3,000 cycles, at which point testing was ceased to continue technology development. The panel reaches a steady state response after 800 cycles and the greatest decrease in stiffness occurred in the first 10 cycles; catastrophic failure was never observed [9]. In addition to a global drop in opening force, the damage caused in the first 10 cycles is also manifested geometrically as, once opened, the panel does not return to its full closed configuration. To ensure better radiation shielding in the (not fully) closed configuration, thin aluminum sheets are adhered to the free ends of the composite panel.

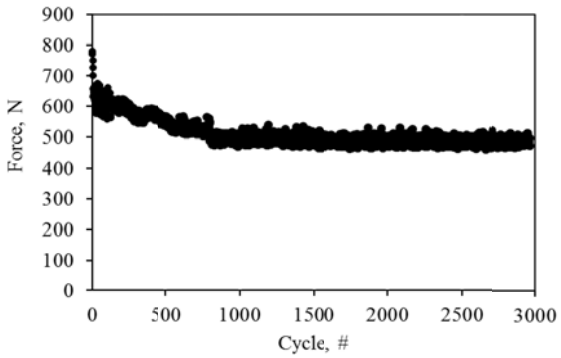

Figure 7: Pull force of radiator panel vs. cycle number.

4 SHAPE MEMORY ALLOY WIRES

4.1 ALLOY TRAINING

Full radiator closure is essential to system performance as it dictates turndown; however, it has proven difficult to achieve in past morphing radiator efforts [**?**]. In this effort, a Nickel-Titanium-Hafnium (NiTiHf) alloy and a Nickel-Titanium-Palladium (NiTiPd) alloy were developed by NASA Glenn Research Center in pursuit of transition temperature goals for the morphing radiator [9]. The SMAs were trained at Texas A&M until sufficiently stable. SMA wire training consists of thermal cycling at maximum expected stress through temperatures 20°C below the Martensite finish temperature (M_f) and 20°C above Austenite finish temperature (A_f). Training was done in an electromechanical load frame system (MTS Insight) inside an environmental chamber (AEC). Custom-built load frame grips allow for continuous SMA wire looping in a pulley-like fashion, uniformly distributing load across the vertical sections of multiple SMA wires, depicted in Figure 8. Such a setup allows for twelve equivalent lengths of wire to be trained simultaneously. The alloys were considered to be sufficiently stable when their transition temperatures changed by less than 1 °C after cycling at the highest expected stress (200 MPa). The chosen alloys underwent eight thermal cycles before demonstrating sufficient stability, as depicted in Figure 9. Once stable, the SMA wires are expected to behave consistently in any application for which the operational stress does not exceed the training stress, which is the case in the current SMA/composite assembly [9].

Figure 8: SMA wire training setup for twelve equivalent lengths of wire.

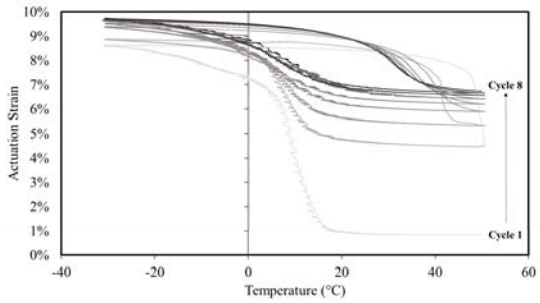

(a) NiTiHf thermal cycling response.

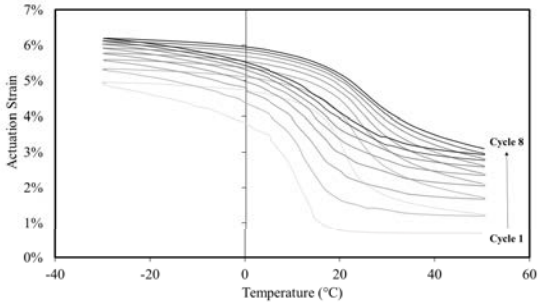

(b) NiTiPd thermal cycling response

Figure 9: SMA thermal cycling response during training.

The final transition temperatures were determined from the response of the trained material. The morphing radiator panel undergoes a variable load. The wires experience no load while the panel is in a fully closed configuration and a maximum load in the fully open configuration. To understand the transition temperatures at different open or closed positions, both alloys were characterized at the smallest load possible while keeping the wire in tension using the setup depicted in Figure 8 (22 MPa) and at maximum expected loads (200 MPa). Using the trained response of the material, tangent lines to the strain vs. temperature curve drawn at the coldest and warmest temperatures during transition and recovery of the material, approximate distinct intersections that provide the transition temperatures of the alloy, depicted as an example in Figure 10.

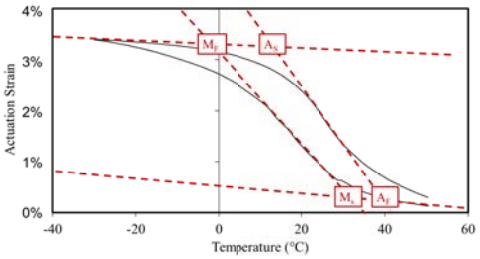

Figure 10: NiTiPd trained material response with tangent lines displaying transition temperatures.

The experimentally estimated phase diagram for each alloy is depicted in Figure 11. The colored lines schematically indicate the actuation of the morphing radiator, limited by the working fluid temperature limits depicted as the gray boundaries.

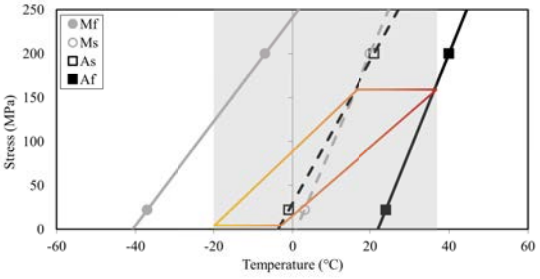

(a) NiTiHf phase diagram.

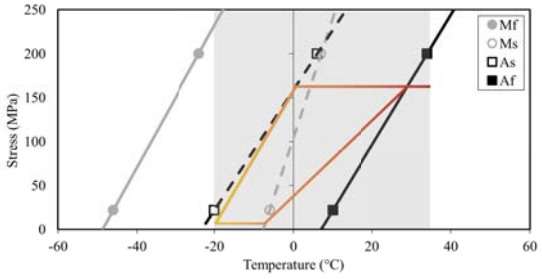

(b) NiTiPd phase diagram.

Figure 11: Experimentally estimated phase diagram for developed alloys.

5 DEMONSTRATION

Thermal chamber testing was performed at Texas A&M University as a preliminary demonstration of full system actuation. The system (5 units) was placed in an environmental chamber and cycled between -30°C and 50°C. All 5 panels were observed to reach full closure (the aluminum sheets on each panel touching). The full open and full closed radiator states as seen during thermal chamber testing are depicted in Figure 12.

Thermal Vacuum Chamber (TVAC) testing was then performed in Chamber N at NASA Johnson Space Center with the goal of characterizing response in a relevant environment for performance verification and technology readiness level progression. A chiller with 50/50 Ethylene Glycol Water (EGW) mixture was pumped through a pipe conductively coupled to the morphing radiators, providing inlet fluid temperature control. Resistance temperature devices (RTDs) were placed in the flow between each morphing radiator unit to measure the temperature at each radiator inlet and outlet while a high accuracy coriollis meter measured the flow rate of the fluid. This instrumentation allows for the heat to and from the fluid $\dot{Q}_{fl}$ can be calculated for each morphing radiator via

$$\dot{Q}_{fl} = \dot{m} c_p (T_{fl,out} - T_{fl,in}), \tag{3}$$

where $\dot{m}$ is the mass flow rate acquired by the coriolis meter, c_p is the specific heat of the fluid calculated as the ideal specific heat of the EGW at the mean fluid temperature, and $(T_{fl,out} - T_{fl,in})$ is averaged transient data from the RTDs for each radiator [9]. From this, the turndown for the morphing radiator can be calculated using equation 2.

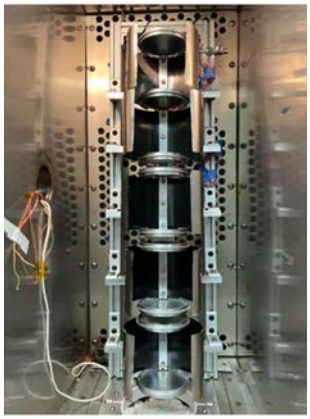

(a) Fully open radiator panels.

(b) Fully closed radiator panels.

Figure 12: Radiator panels as observed in thermal chamber testing at Texas A&M University.

6 RESULTS

Thermal Vacuum Chamber (TVAC) testing was performed for a total of 97 hours. Testing of the 5-panel system and that of a single morphing radiator was performed. Overall, the best heat flux and turndown observed during the testing campaign was 304 W/m2 and 8.9:1, respectively, during testing of a single panel (Figure 13) [9].

7 CONCLUSION

Lifetime cycling of the morphing radiator panel demonstrated performance to 3,000 cycles, representing 2,600 more cycles than previous benchtop demonstrations. Development of the fatigue test stand allowed for understanding of the radiator composite fatigue properties and is imperative for further development.

The morphing radiator achieved the highest turndown for a morphing radiator concept to

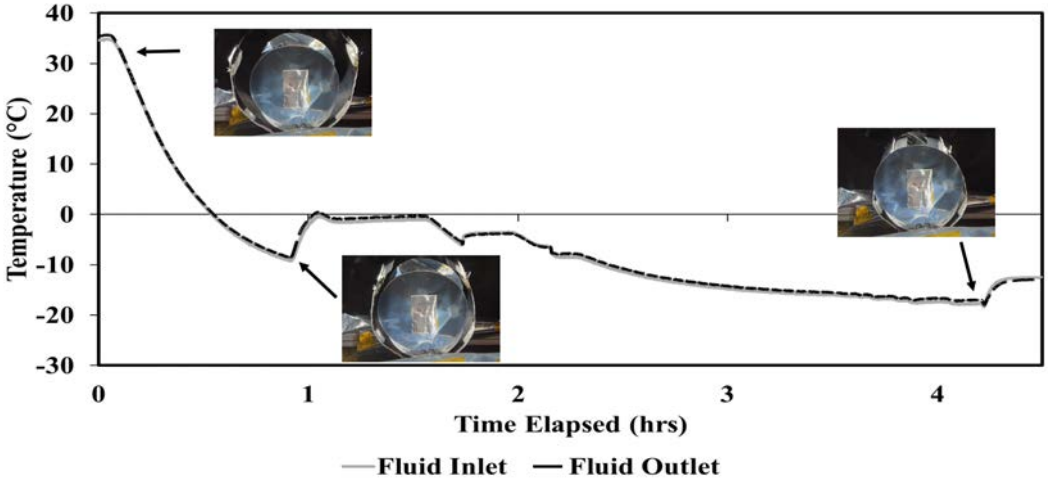

Figure 13: Single panel TVAC test temperature results.

date with a turndown of 8.9:1, greater than NASA's 2015 technology roadmap goal of 6:1. With a 5-panel system assembly, the system includes the highest number of morphing radiators in series tested in a vacuum chamber to date. This work demonstrates progression of the morphing radiator characterization. Successful testing of a five unit system in a relevant environment increases the technology readiness level of the morphing radiator to TRL 5. Most importantly, the morphing radiator allows for the use of a single loop TCS, which is lighter and less complex than a dual loop TCS, without the risk of fluid freeze.

8 ACKNOWLEDGEMENTS

The authors would like to acknowledge the support of Daniel C. Miller and Connor Joyce from Paragon Space Development Corporation, Othmane Benafan from NASA Glenn Research Center, and Sean Nevin from The Boeing Company. Doug Nicholson of The Boing Company was the lead researcher on an SMA-driven thermal switch associated with the radiator concept but not addressed herein.

REFERENCES

[1] D. J. Miranda, A. Conde, and D. A. Terrier, "The 2020 NASA technology taxonomy," in *Proceedings of the International Astronautical Congress, IAC*, vol. 2019-October, 2019.

[2] T. L. Bergman, A. S. Lavine, F. P. Incropera, and D. P. Dewitt, *Fundamentals of Heat and Mass Transfer, 2011. Fundamentals of Heat and Mass Transfer. 7th Edition.*, 2011.

[3] T. O. Leimkuehler and G. Lantz, "Single loop thermal control for deep space exploration," in *42nd International Conference on Environmental Systems 2012, ICES 2012*, 2012.

[4] D. A. Ochoa, V. Walt, and M. K. Ewert, "A comparison between one-and two-loop atcs architectures proposed for CEV," *SAE International Journal of Aerospace*, vol. 4, no. 1, 2011.

[5] D. C. Lagoudas, *Shape Memory Alloys: modeling and engineering applications.* Springer, 2008.

[6] C. L. Bertagne, T. J. Cognata, R. B. Sheth, C. E. Dinsmore, and D. J. Hartl, "Testing and analysis of a morphing radiator concept for thermal control of crewed space vehicles," *Applied Thermal Engineering*, vol. 124, 2017.

[7] C. L. Bertagne, J. B. Chong, J. D. Whitcomb, D. J. Hartl, and L. R. Erickson, "Experimental characterization of a composite morphing radiator prototype in a relevant thermal environment," in *25th AIAA/AHS Adaptive Structures Conference, 2017*, 2017.

[8] P. Walgren, S. Nevin, and D. Hartl, "Design, experimental demonstration, and validation of a composite morphing space radiator," *Journal of Composite Materials*, vol. 57, no. 3, pp. 347–362, 2023.

[9] D. Miller, C. Joyce, D. Hartl, P. Nizio, D. Nicholson, S. Nevin, O. Benafan, G. Biglow, and D. Gaydosh, "Shape Memory Alloys for Regulating TCS in Space (SMARTS): System Design and Thermal Vacuum," in *51st International Conference on Environmental Systems*, St. Paul, 2022.

[10] C. Bertagne, P. Walgren, L. Erickson, R. Sheth, J. Whitcomb, and D. Hartl, "Coupled behavior of shape memory alloy-based morphing spacecraft radiators: Experimental assessment and analysis," *Smart Materials and Structures*, vol. 27, no. 6, 2018.

[11] S. Nevin, *Combined Thermal and Structural Modeling and Design of a Shape Memory Alloy Driven Morphing Space Radiator (Ms thesis).* College Station: Texas A&M University, 12 2021.